



Validation of brightness and physical temperature from two scanning microwave radiometers in the 60 GHz O₂-band using radiosonde measurements

Francisco Navas-Guzmán¹, Niklaus Kämpfer¹, and Alexander Haeefe²

¹Institute of Applied Physics (IAP), University of Bern, Bern, Switzerland

²Federal Office of Meteorology and Climatology MeteoSwiss, Payerne, Switzerland

Correspondence to: Francisco Navas-Guzmán (francisco.navas@iap.unibe.ch)

Abstract.

In this paper, we address the assessment of the tropospheric performance of a new temperature radiometer (TEMPERA) at 60 GHz. With this goal, an intercomparison campaign was carried out at the aerological station of MeteoSwiss in Payerne (Switzerland). The brightness temperature and the tropospheric temperature were assessed by means of a comparison with simultaneous and collocated radiosondes which are launched twice a day at this station. In addition, the TEMPERA performances are compared with the ones from a commercial microwave radiometer (HATPRO) which has some different instrumental characteristics and uses a different inversion algorithm. Brightness temperatures from both radiometers were compared with the ones simulated using a radiative transfer model and atmospheric profiles from radiosondes. A total of 532 cases were analyzed under all weather conditions and evidenced larger brightness temperature deviations between the two radiometers and the radiosondes for the most transparent channels. Two different retrievals for the TEMPERA radiometer were implemented in order to evaluate the effect of the different channels on the temperature retrievals. The comparison with radiosondes evidenced better results and very similar to the ones from HATPRO when the 8 more opaques channels were used. The study shows the good performance of TEMPERA to retrieve temperature profiles in the troposphere. The inversion method of TEMPERA is based on the Optimal Estimation Method. The main advantage of this algorithm is that there is no necessity for radiosonde information to achieve good results in contrast to conventional methods as neuronal networks or lineal regression. Finally, an assessment of the effect of instrumental characteristics as the filter response and the antenna pattern on the brightness temperature showed that they can have an important impact on the most transparent channels.

1 Introduction

The importance of the knowledge of the thermal structure for scientific understanding of atmospheric processes is widely recognized. The air temperature plays a crucial role on the dynamical, chemical and radiative processes in the atmosphere. In the lowest part of the atmosphere, temperature profiles are a key input for the weather forecast models. Techniques based on in-situ or remote sensing measurements are used nowadays to measure atmospheric temperature profiles. Among the in-situ techniques, radiosondes are extensively used due to high spatial resolution. Recently, the global Aircraft Meteorological DATA



Relay (AMDAR) programme initiated by the World Meteorological Organization (WMO) and its Members is using aircraft temperature measurements for a range of meteorological applications (public weather forecasting, climate monitoring and prediction, etc). The aircraft use sensors or the emerging MODE-S method to retrieve the temperature. The main disadvantage of these in-situ techniques is their high cost and a very low temporal resolution. Other measurement techniques have become available to address the necessity of temperature measurements in the troposphere and in the stratosphere. These measurements include lidar and microwave radiometers. Microwave radiometers present as main advantage the capacity of providing atmospheric profiles with a high temporal resolution and a reasonable spatial resolution. In addition, long-term measurements in a fixed location allow to characterize the local atmospheric dynamics.

At the present there are different configurations of ground-based microwave radiometers to measure tropospheric temperature profiles, some examples are MICCY (microwave radiometer for cloud cartography) (Crewell et al., 2001), Radiometrics MP-3000A (Ware et al., 2003), RPG-HATPRO (Radiometer Physics GmbH-Humidity and Temperature Profiler) (Rose et al., 2005) and ASMUWARA (All-Sky MUltiWavelength RAdiometer)(Martin et al., 2006).

A relatively new temperature radiometer (TEMPERA) has been designed and built by the microwave group at the Institute of Applied Physics (IAP), University of Bern, Switzerland. This is the first ground-based radiometer which measures temperature profiles in the troposphere and in the stratosphere simultaneously (Stähli et al., 2013; Navas-Guzmán et al., 2014).

The presented study tries to assess the tropospheric performance of TEMPERA radiometer comparing with independent in-situ radiosonde measurements. TEMPERA has also been compared with a commercial microwave radiometer (HATPRO) manufactured by Radiometer Physics GmbH, Germany (RPG). This second radiometer has some different technical characteristics and the inversion algorithm is based on a different method. Most of the temperature inversion algorithms used for commercial radiometers are based on neuronal networks or linear regression methods which suffer from the need of using radiosondes to train that method. The difficulty in the availability of a statistical significant radiosonde database for the location of the microwave radiometer is one of the major drawbacks of these methods. In this sense, the TEMPERA's inversion algorithm based on the Optimal Estimation Method (OEM) (Rodgers, 2000) overcomes this problem. In addition to the temperature assessment the radiances measured from both radiometers (brightness temperatures) will be evaluated. For that purpose the brightness temperature (T_b) from both radiometers are compared with the simulated T_b from radiosondes using a radiative transfer model. Finally, this study also tries to assess how some instrumental characteristics as the filter responses and the antenna pattern affect the measured radiances (brightness temperature).

The paper has been organized in the following way. Section 2 presents the experimental site and the instrumentation used in this study. Section 3 describes the methodology of the radiative transfer model and the temperature inversions. Section 4 and 5 present the brightness and physical temperature comparisons carried out for one year of measurements. An assessment of the effect of radiometer characteristics as the filter response and the antenna pattern on the brightness temperature is presented in section 6. Finally the conclusions are found in section 7.



2 Experimental site and instrumentation

A special campaign has been set up at the aerological station in Payerne (46.82 N, 6.95 E; 491 m above sea level) of the Swiss Federal Institute of Meteorology and Climatology (MeteoSwiss). For this campaign TEMPERA radiometer was moved from the ExWi building of the University of Bern (Bern, Switzerland) to Payerne in December of 2013. The main goal of this campaign is to assess the tropospheric and stratospheric performance of TEMPERA using the versatile instrumentation available at this MeteoSwiss station. Particular, in this study we will assess the brightness temperature and the tropospheric temperature profiles comparing with the radiosondes which are launched twice per day at this station. In addition, the performance of TEMPERA are compared with another microwave radiometer (HATPRO), which has some different instrumental characteristics and also uses a different inversion algorithm. Next a technical description of the different instruments used in this study is presented.

The temperature radiometer called TEMPERA has been designed and built by the Institute of Applied Physics (IAP) of the University of Bern (Stähli et al., 2013). Figure 1 shows a picture of this radiometer at the laboratory at ExWi, Bern (Switzerland). TEMPERA is a heterodyne receiver which covers the frequency range of 51-57 GHz. The instrument consists of a frontend to collect the microwave radiation and two backends for the detection (a filter bank and a Fast Fourier Transform spectrometer (FFT)). The incoming radiation is directed into a corrugated horn antenna using an off-axis parabolic mirror. The antenna is characterized by a Half Power Beam Width (HPBW) of 4° . The calibration of the detected signal in the two backends is performed by means of an ambient hot load in combination with a noise diode.

The tropospheric measurements in TEMPERA are performed using the filter bank. It consists of 4 filters which are able to measure at 12 frequencies by tuning the frequency of a local oscillator (LO) with a synthesizer. Thus, the positions between the emission lines in the 51-57 GHz range are covered uniformly (see Fig. 2). Filters with different bandwidths are used to measure at the 12 frequencies, while for lower 9 channels the filters' bandwidths are 250 GHz for the 3 more opaque channels (10-12) wider ones (1 GHz) are used in order to enhance the sensitivity in the flat spectral region. Table 1 shows the central frequencies and the bandwidths of all the channels. For tropospheric measurements a scanning is performed by TEMPERA in every measurement cycle covering the elevation angle range from 20° to 60° in steps of 5° (9 angles). Crewell and Lohnert (2007) showed that these elevation scanning measurements increase the accuracy of the retrieved temperature, specifically in the boundary layer, for microwave radiometers.

For the stratospheric temperature retrievals TEMPERA uses the second backend (FFT spectrometer, Acquiris AC 240) to measure the two oxygen-emission lines centered at 52.5424 and 53.0669 GHz. Stratospheric measurements are not treated in this paper and a detailed description of this other measurement mode can be found in Stähli et al. (2013) and Navas-Guzmán et al. (2015).

TEMPERA performs periodic measurement cycles of 60 s. Each cycle starts with a hot load calibration in combination with a noise diode followed by the atmosphere measurements (scanning from 60° to 20° elevation angle in steps of 5°). After calibration, the output of each measurement cycle is a set of 108 brightness temperatures corresponding to the 12 frequencies

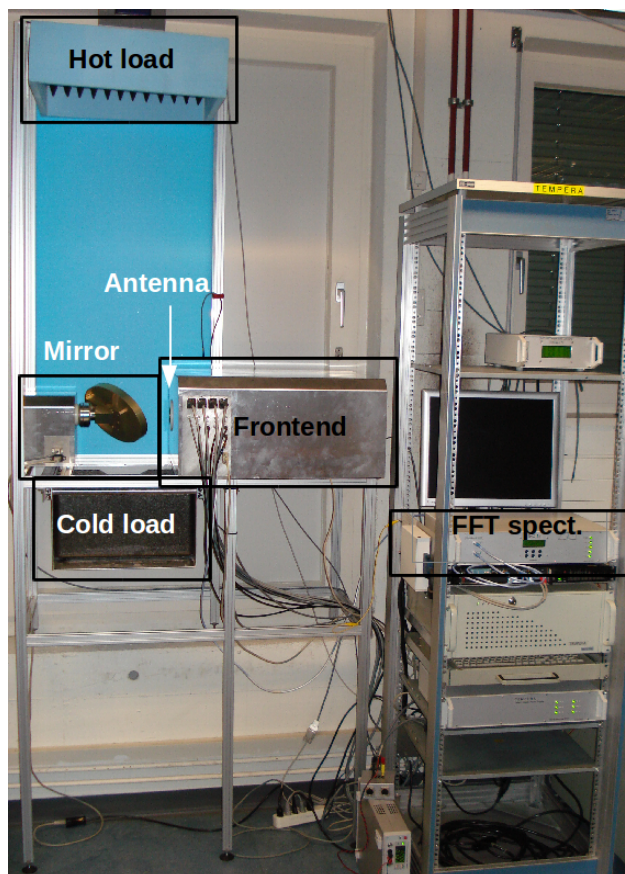


Figure 1. TEMPERA at the laboratory at ExWi, Bern (Switzerland).

Table 1. Frequencies (f) and bandwidths (B) of TEMPERA's tropospheric channels (ch1-ch12).

channel	f [GHz]	B [MHz]	channel	f [GHz]	B [MHz]
1	51.25	250	7	54.40	250
2	51.75	250	8	54.90	250
3	52.25	250	9	55.40	250
4	52.85	250	10	56.00	1000
5	53.35	250	11	56.50	1000
6	53.85	250	12	57.00	1000

and the 9 elevation angles. The noise diode is calibrated regularly (about once a month) using a cold load (liquid nitrogen) and a hot load (ambient). The time resolution of these retrievals is 15 min (Stähli et al., 2013).

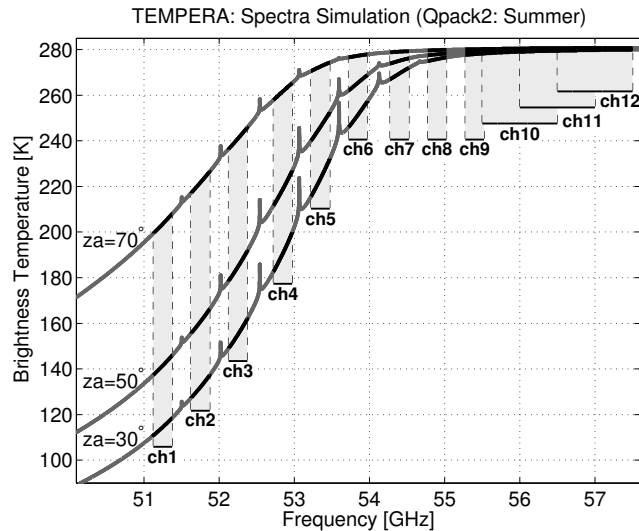


Figure 2. Simulated brightness temperatures using ARTS model for HATPRO radiometer at different zenith angles (30° , 50° and 70°). The grey bars indicate the 12 channels of the filterbank.

The other microwave radiometer used in the study is a HATPRO radiometer (RPG-HATPRO, Radiometer Physics GmbH) (Rose et al., 2005). This instrument provides very accurate values of Liquid Water Path (LWP) and Integrated Water vapour (IWV) with a high temporal resolution (1s). Measurements in the bands 22-31 GHz and 51-58 GHz make possible to retrieve humidity and temperature profiles with this radiometer. HATPRO measures the sky brightness temperature at six elevation angles (90.0° , 42.0° , 30.0° , 19.2° , 10.2° and 5.4°) corresponding to 1.0, 1.5, 2.0, 3.0, 5.6 and 10.6 air masses in a continuous and automated way with a radiometric resolution between 0.3 and 0.4 K root mean square error at 1.0 s integration time. Whereas the first band provides highly accurate information of humidity and cloud liquid water content (Löhnert and Crewell, 2003), the second band contains information about the tropospheric vertical structure of the temperature due to the homogeneous mixing of O_2 (Crewell and Lohnert, 2007). HATPRO uses two filter banks in order to detect the radiation coming from both bands in parallel. For temperature retrievals seven channels are used at the frequencies 51.26, 52.28, 53.86, 54.94, 56.66, 57.30 and 58.00 GHz. The lower four channels have a bandwidths of 230 MHz while for the optically thick channels (56.66-58 GHz) wider bandwidths (2 GHz) are used.

Independent in-situ temperature measurements are taken by means of radiosondes. Radiosondes are regularly launched twice a day at the aerological station of Payerne since 1954. They typically reach altitudes around 30 km, with a spatial resolution which range between 10 to a maximum of 80 m with a highest resolution in the first seconds of the flight. The sensors of these radiosondes include copper-constantan thermocouples for temperature, a full range water hypsometer for pressure, and a carbon hygistor for relative humidity. The accuracies of these three parameters in the troposphere are ± 0.2 K for temperature, ± 2 hPa (accuracy increases with height) for pressure and ± 5 to 10% for relative humidity (Löhnert and Maier, 2012).



3 Methodology

TEMPERA and HATPRO radiometers measure thermal radiation in the range from 51 to 58 GHz coming from the wing of the 60 GHz oxygen-emission region. For a well mixed gas such as oxygen, whose fractional concentration is altitude independent below 80 km, the radiation provides information firstly on atmospheric temperature.

- 5 A microwave radiometer measures atmospheric thermal emissions coming from different altitudes. The intensity of the radiation detected at ground level can be calculated as a function of the frequency dependent microwave brightness temperature (Tb). Under the Rayleigh-Jeans approximation ($h\nu \ll kT$) the radiative transfer equation is expressed as

$$Tb(h_0, \theta) = T_0 e^{-\tau(h_1, \theta)} + \int_{h_0}^{h_1} T(h) e^{-\tau(h, \theta)} \alpha \frac{1}{\cos(\theta)} dh \quad (1)$$

- where $Tb(\theta)$ is the brightness temperature at zenith angle θ , T_0 is the brightness temperature of the cosmic background radiation, $T(h)$ is the physical temperature at height h , h_0 is the altitude at ground, h_1 is an upper boundary in the atmosphere, α is the absorption coefficient and τ is the opacity. The opacity is defined as

$$\tau(h, \theta) = \int_{h_0}^h \alpha(h') \frac{1}{\cos(\theta)} dh' \quad (2)$$

- The estimated brightness temperature can be easily calculated from equation 1 just knowing the state of the atmosphere (forward model). However, a much more complex task is to solve the inverse problem: what is the physical temperature profile which give rise to the measured brightness temperature. This is an ill-posed problem and the solution is under-constrained.

- Two different inversion methods have been used in this study. The temperature retrievals for TEMPERA radiometer are based on the Optimal Estimation Method (OEM) (Rodgers, 2000). The measured brightness temperatures are inverted to temperature profiles using the ARTS/QPack software package (Eriksson et al., 2011). More information about this method applied to TEMPERA measurements can be found in Stähli et al. (2013). For these retrievals, the absorption coefficients used in the radiative transfer calculations for the different species are obtained from the Rosenkranz and Liebe models: Rosenkranz (1993) for O_2 , Liebe et al. (1993) for N_2 and Rosenkranz (1998) for H_2O . A tropospheric water vapour profile is also included in the forward model. The profile is obtained from the measured surface water vapour density at ground (from a weather station) and assuming an exponential decrease with the altitude of the water vapour and a scale height of 2 km (Bleisch et al., 2011). Standard atmospheric profiles for summer and winter are considered for other species as oxygen (O_2) and nitrogen (N_2), these profiles are incorporated into ARTS2 (middle latitude FASCODE (Fast Atmospheric Signature CODE) (Anderson et al., 1986)).

The retrievals for HATPRO measurements are based on a linear regression method. This algorithm uses simulated Tbs at required frequencies and elevation angles derived from 17 years of atmospheric radiosonde profiles at Payerne and radiative transfer calculations. The statistical multi-linear regression coefficients are obtained from the comparison between the tem-



perature profiles and the simulated Tb_s data set from the radiosondes. For the HATPRO temperature retrievals, the brightness temperature measured at the V-band frequencies are used, where the first 3 frequencies are only used in zenith pointing (51.26, 52.28 and 53.86 GHz) and the last 4 (54.94, 56.66, 57.3 and 58 GHz) are considered for all the elevation angles (Meunier et al., 2013). More detail about the atmospheric profiles and the absorption models used in the radiative transfer model can be found
5 in Löhnert and Maier (2012).

4 Brightness temperature comparison

The measured Tb from both radiometers (TEMPERA and HATPRO) have been compared with the ones simulated using radiosonde (RS) measurements. The simulated Tb from RS were calculated using the Atmospheric Radiative Transfer Simulator (ARTS, (Eriksson et al., 2011; Buehler et al., 2005)) which implement the Radiative Transfer Equation (RTE) presented in Eq.
10 1. In the radiative transfer calculations we use the models of Rosenkranz and Liebe for the absorption coefficient calculations: Rosenkranz (1998) for H_2O , Rosenkranz (1993) for O_2 and (Liebe et al., 1993) for N_2 . The input to the model consists of an atmospheric sounding, which provides information on pressure, height, temperature, water vapour density and cloud liquid water content (LWC). In this study we have assumed a constant LWC value of 0.28 g/m^3 for those altitudes with a relative humidity larger than 97% and a temperature larger than -20° C . For other species like oxygen and nitrogen we used standard
15 atmospheric profiles for summer and winter (Anderson et al., 1986), which are incorporated into ARTS2.

In the next subsections we present the Tb comparison for one year of measurements (January-December 2014) between ones measured from TEMPERA and HATPRO radiometers and the simulated Tb from RS measurements.

4.1 TEMPERA versus RS

In addition to atmospheric parameters some radiometer characteristics were provided as input of the forward model. These
20 inputs variables include the microwave frequencies, the elevation angles, the filter response and the antenna pattern. Table 1 presents the central frequencies and the bandwidths of the different channels for TEMPERA. A Gaussian beam of 4° of half-power beamwidth (HPBW) has been considered as TEMPERA's antenna pattern in the forward model.

The simulated Tb from RS measurements were calculated using ARTS model for the same elevations angles (12) and frequencies (9) than the ones used by TEMPERA in the tropospheric mode. A total of 532 measurements have been compared
25 along one year of data.

Figure 3 shows the Tb deviation between TEMPERA radiometer and RS at elevation angle of 60° along 2014 for all weather conditions (except rainy cases). The classification of clear and cloudy cases was performed using an automatic partial cloud amount detection algorithm (APCADA) (Dürr and Philipona, 2004). This algorithm determines cloud fraction using longwave downward radiation and surface temperature and humidity measurements with a 10 min resolution. The range goes from 0 octa
30 (clear-sky) to 8 octa (overcast). Clear conditions have been considered for those situations where the number of octas is 0 or 1. Moreover, an additional constraint considered was that the integrated liquid water (ILW) measured from HATPRO radiometer was lower than 0.025 mm. We can observe in Figure 3 that the largest bias in the Tb between TEMPERA and RS are found

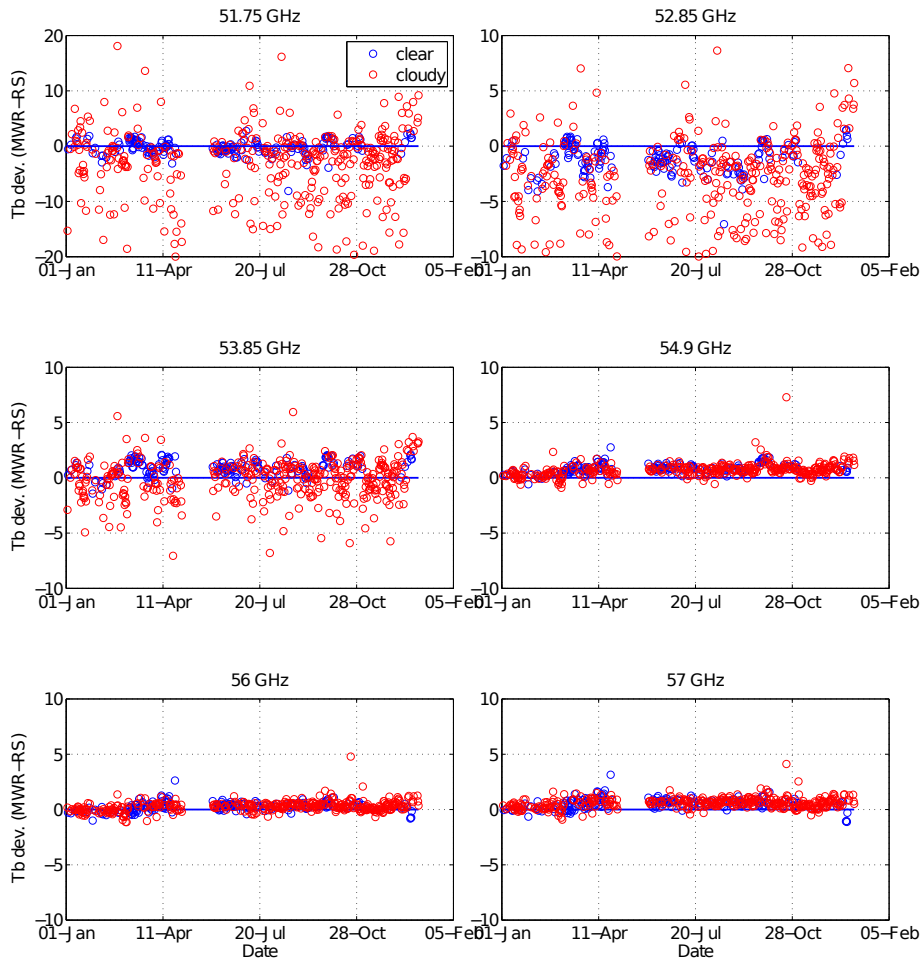


Figure 3. Tb deviation between TEMPERA and RS at 60° elevation angle for 6 frequencies.

for the most transparent channels under cloudy conditions (red circles). For cloudy conditions there are discrepancies that reach almost 20 K for the 51.75 GHz channel. A different behaviour is observed for the most opaque channels where the bias between TEMPERA and RS for both clear and cloudy conditions are much smaller with deviations below 2 K for most of the measurements. The larger bias found for cloudy conditions can be explained by the presence of non homogeneous conditions for many of the cases which produce non comparable measurements for both instruments. Moreover, the simulations of clouds in the forward model is an additional difficulty.

Figure 4a shows the mean Tb deviation between TEMPERA and RS for all the frequencies and elevation angles of TEMPERA radiometer and for all weather conditions. From this plot we can observe that there is a strong dependency with the frequency and the elevation angle. We could clearly separate the deviations between the transparent and the opaque channels.

For the more opaque channels (>53.5 GHz) the agreement between TEMPERA and the RS is quite good with differences



always lower than 1 K for all the elevation angles. For these channels we can observe that there is no strong dependency with the elevation angles. In contrast, the more transparent channels show a strong dependency with the elevation angle and larger differences between TEMPERA and RS. The T_b bias ranges from positive values (1.6 K at 51.25 GHz) for the lowest elevation angle to negative values (-2.8 K at 52.85 GHz) for the largest elevation angle. The change from positive to negative bias when the elevation angle increase could be due to the effect of the clouds in the forward model, suggesting a possible overestimation from the RS when clouds are incorporated to the forward model.

In order to avoid the complexity of cloudy cases which could present inhomogeneous conditions and to assess the T_b bias due to instrumental and modelling aspects cases with clear conditions were only selected. Figure 4b shows the mean T_b deviation between TEMPERA and RS for clear conditions. A total of 160 cases were identified as cloudless using the criteria mentioned above. From this plot we can also observe the strong dependency with the frequency and the elevation angle. The behaviour is similar to the plot with all weather conditions, finding the largest differences for the most transparent channels. For the more opaque channels (>53.5 GHz) the T_b bias ranges between 1.3 K (elev. angle = 30° , freq. = 53.85 GHz) and 0.2 K (elev. angle = 45° , freq. = 56 GHz). For the more transparent channels it is worth to point out that for most of the channels and elevation angles there is a positive bias between the measured T_b from TEMPERA and the one simulated from RS. We can see that the bias is larger for the lower elevation angles. The bias ranges between 4.63 K (elev. angle = 20° , freq. = 51.25 GHz) and -1.1 K (elev. angle = 60° , freq. = 52.85 GHz). In Table 2 we can find the mean T_b deviations and the standard deviations for 5 channels and all the elevations angles for clear conditions. Similar and even larger systematic offsets have been found in the more transparent V-band channels in other studies where radiometers from different manufacturers were used (Löhnert and Crewell, 2003; Hewison et al., 2006). The standard deviation of the T_b offsets (Table 2) is lower than 0.75 K for the channels that are more optically thick. However, the more transparent channels show temporal variations of the T_b offsets up to 1.73 K. The larger variability in the more transparent channels could be explained by a possible temporal shift between the radiosonde and the MWR measurements since both techniques have different integration times and/or that both instruments sounded very different air masses (due to the vertical sonde drift). In addition, uncertainties in the oxygen absorption model as well as the radiometric noise could explain these variations (Löhnert and Maier, 2012).

4.2 HATPRO radiometer versus RS

The measured T_b from HATPRO radiometer was also compared with the ones simulated using RS measurements. For this new comparison the ARTS model was set with the radiometer instrument characteristics from HATPRO. The seven frequencies (51.26, 52.28, 53.86, 54.94, 56.66, 57.30 and 58.00 GHz) and the six elevation angles (90.0, 42.0, 30.0, 19.2, 10.2 and 5.4) of HATPRO were used as inputs of the forward model. The simulations were performed considering a pencil beam since there was no information about the antenna patter of this radiometer available. In this study, the shape of the filter bandwidth is idealised to a rectangular function with the width specified by the manufacturer (230 MHz for the 4 most transparent channels, 600 MHz at 56.66 GHz, 1 GHz at 57.30 GHz and 2 GHz at 58 GHz).

Figure 5a shows the mean T_b deviations between HATPRO and RS for the seven frequencies and the 6 elevation angles of HATPRO radiometer. The plot presents the deviation for all weather conditions (532 cases). We can observe a positive T_b

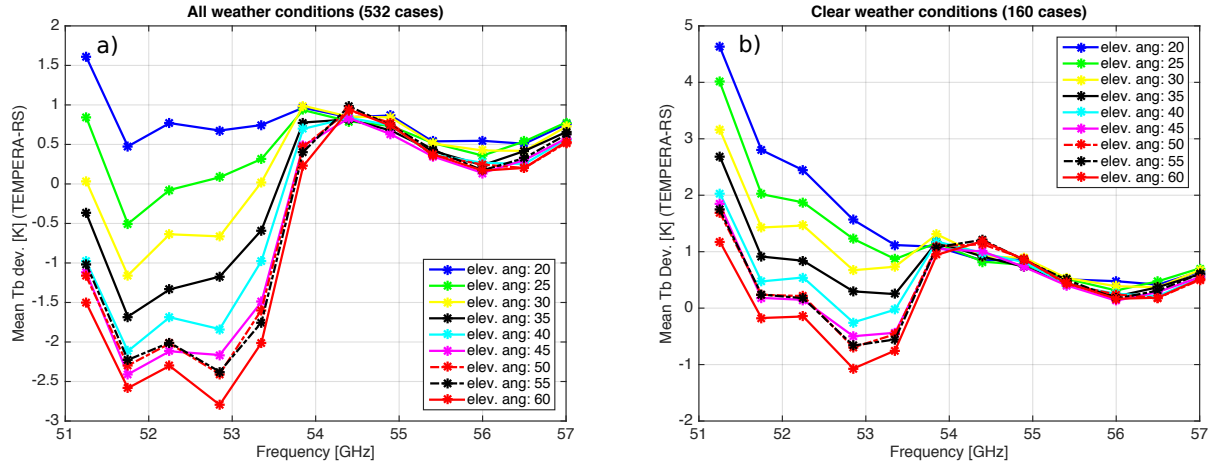


Figure 4. a) Mean T_b deviation between TEMPERA and RS for all weather conditions (532 cases). b) Mean T_b deviation between TEMPERA and RS only for clear conditions (160 cases).

Table 2. Mean T_b and standard deviation between TEMPERA and RS for clear conditions.

elev. angle/ freq.	51.25 GHz	52.25 GHz	53.35 GHz	54.90 GHz	56.50 GHz
20°	4.63/1.73	2.44/1.08	1.12/0.51	0.87/0.55	0.43/0.73
25°	4.01/1.70	1.87/1.26	0.87/0.61	0.77/0.51	0.49/0.68
30°	3.16/1.73	1.46/1.37	0.73/0.72	0.89/0.47	0.39/0.62
35°	2.69/1.67	0.84/1.41	0.25/0.80	0.73/0.45	0.40/0.58
40°	2.03/1.63	0.54/1.43	-0.03/0.89	0.81/0.45	0.24/0.56
45°	1.84/1.53	0.15/1.41	-0.44/0.95	0.73/0.44	0.32/0.54
50°	1.69/1.47	0.21/1.40	-0.46/0.99	0.88/0.42	0.22/0.50
55°	1.74/1.42	0.17/1.38	-0.56/0.99	0.85/0.43	0.35/0.51
60°	1.18/1.38	-0.15/1.36	-0.75/1.03	0.86/0.43	0.23/0.49

offset between HATPRO and the RS for all the frequencies and elevation angles except the second one (52.28 GHz). The T_b bias ranges between 3.6 K at 53.86 GHz and the zenith pointing to -6.3 K at 52.28 GHz and the elevation angle of 42°. In order to avoid possible inhomogeneous conditions due to the clouds we have again selected clear cases for the comparison. Figure 5b shows the deviations for these conditions. We observe again that there is a strong dependency with the elevation angles for the more transparent channels, but in this case the second channel (52.28 GHz) evidences a very different behavior than the other ones. A positive offset is observed in all the channels except for the second one. The T_b bias ranges between 5.3 K for the more transparent channels at 30° of elevation angle and -4.5 K for the second channel (52.28 GHz) at the zenith observation.



For the more opaque channels (≥ 54.94 GHz) the dependency with the elevation angle is weaker and shows a positive offset which range between 0.8 and 1.6 K.

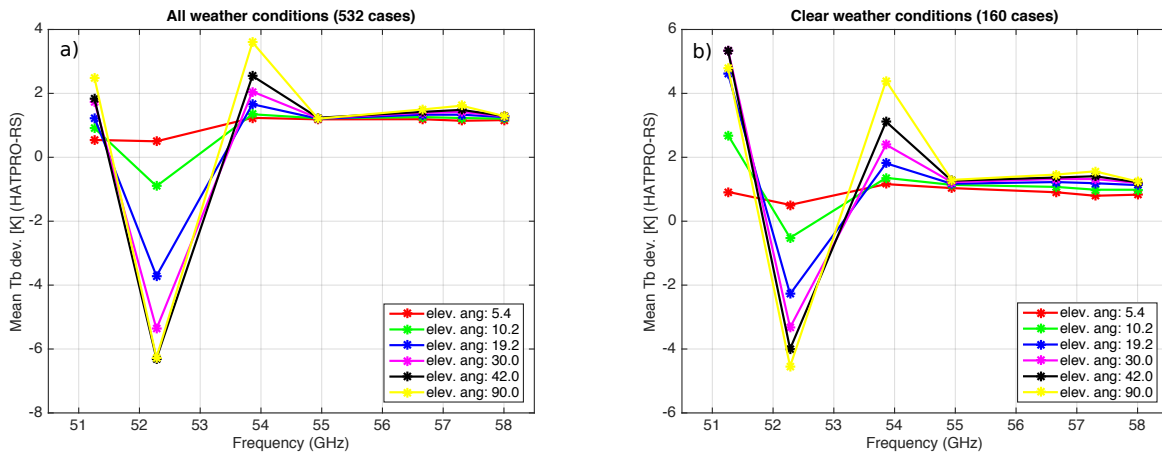


Figure 5. a) Mean T_b deviation between HATPRO and RS for all weather conditions (532 cases). b) Mean T_b deviation between HATPRO and RS only for clear conditions (160 cases).

Table 3 presents the mean and the standard T_b deviation between HATPRO and the radiosondes for the more opaque channels and all elevation angles. The largest standard deviation (2.1 K) is found for the most transparent channel at the elevation angle of 19.2° . A similar comparison study between the same radiometer and RS was performed by Löhnert and Maier (2012) for more than 3 years of measurements at Payerne. Similar mean and standard deviations were found for the more transparent channels in that study. In contrast, the other channels presented lower mean T_b deviations than in this study for the different elevation angles. It is also worth to remark that the largest mean T_b deviations are found for the larger elevation angles (larger than 19°) for both studies. One of the possible reasons that could explain these large discrepancies (larger than for TEMPERA) is that for HATPRO radiometer are not known the exact center frequencies and band passes for the instrument analysed in this study (Löhnert and Maier, 2012). Meunier et al. (2013) studied the impact of the radiometer characteristics (e.g., antenna beam width and receiver bandwidth) on scanning radiometer measurements and they found that a non appropriate characterization of the bandwidth could lead to errors up to 8 K in the V-band. The errors are more important in the vicinity of absorption peaks.

5 Intercomparison of retrieved temperature profiles

Physical temperature profiles retrieved from both MWRs are also compared with independent in-situ temperature measurements from RS for one year of data (2014). A total of 532 coincident cases were inverted corresponding to all weather conditions (except rainy cases). As it was already indicated in section 3 different inversion algorithms were used to retrieve temperature profiles from the two radiometers.



Table 3. Mean T_b and standard deviation between HATPRO and RS for clear conditions.

elev. angle / freq.	51.26 GHz	52.28 GHz	53.86 GHz	54.94 GHz
5.4°	0.92/0.68	0.51/0.37	1.16/0.53	1.04/0.73
10.2°	2.69/1.78	-0.52/0.84	1.36/0.38	1.14/0.53
19.2°	4.61/2.10	-2.28/1.47	1.81/0.34	1.17/0.39
30°	5.35/1.84	-3.33/1.56	2.40/0.46	1.22/0.34
42°	5.33/1.60	-4.00/1.51	3.11/0.62	1.27/0.35
90°	4.79/1.25	-4.55/1.31	4.39/0.85	1.29/0.40

The temperature retrievals for TEMPERA are based on the Optimal Estimation Method (OEM) and have been performed using ARTS/qpac package (Eriksson et al., 2011). The method needs an apriori temperature profile in order to constrain the solutions to physically meaningful results. As apriori-profile, monthly mean temperature profiles calculated from 18 years (1994-2011) of daytime radiosonde profiles at Payerne are used. Two different retrievals have been obtained for the TEMPERA measurements. In the first retrievals the brightness temperatures for all the frequencies (12 channels) were used while in the second one only the 8 more opaque channels were considered (frequencies > 53 GHz). These two configurations were used in other studies to deal with clouds, using only the second retrievals (8 channels) when there was presence of clouds. It is well known that clouds have a relatively strong influence in the frequency range from 51 to 53 GHz (Stähli et al., 2013).

In order to perform the comparison between both radiometers and RS all the measurements have been interpolated to the altitude grid of TEMPERA. Figure 6 shows the temperature evolution for the RS, TEMPERA (both inversions) and HATPRO radiometer at different altitudes along 2014. The apriori temperature used for the TEMPERA retrievals has also been plotted. We can observe that in general there is a very good agreement between RS and the retrievals from both radiometers. Both radiometers are able to follow the temperature evolution measured by the RS along the year, even if strong temperature changes are observed in a short time period. This plot shows the capability of MWR measurements to measure temperature profiles under very different atmospheric conditions. The highest discrepancies with the RSs are observed in the highest altitudes, particularly for the TEMPERA retrievals with 12 channels (blue line).

Figure 7a shows the BIAS and the standard deviation between the retrievals from both MWRs and the RS for all-sky conditions. Very similar values of mean deviations are found between both retrievals from TEMPERA (with 8 and 12 channels) and the RS in the lowest troposphere (from ground to 1 km agl). Their values range between 0.24 and 0.86 K. For this altitude range the standard deviation also shows almost identical values, which range between 0.8 and 1.4 K. Larger offsets and standard deviations are found for both retrievals in the upper layers. The temperature deviation at ground level present a larger deviation and is not considered in this discussion. This value could be improved for the future considering as ground temperature the measurement from a temperature sensor co-located with TEMPERA as HATPRO radiometer does. Between 1 and 2 km above ground the mean deviation shows very different values for the two retrievals. The one retrieved from 8 channels (8f-RET) presents offsets between 0.8 and 1.1 K while the one from 12 channels (12f-RET) evidence larger deviations (from 1.1 to 2 K). Also the standard deviations are larger for the second retrievals, around 1.5 K for the 8f-RET and around 1.7 K for the

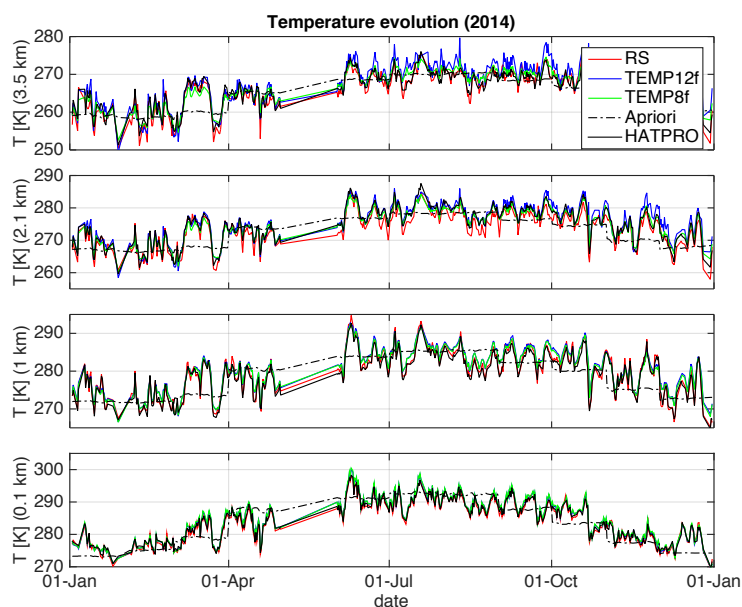


Figure 6. Temperature evolution at different altitudes for RS, HATPRO, TEMPERA (inversions with 8 and 12 filters) and the apriori temperature used for TEMPERA inversions.

12f-RET. Above 2 km the bias for 8f-RET is much lower than the one for 12f-RET. The mean deviation ranges from 0.4 to 1.2 K and from 1.5 to 2.4, respectively, decreasing the offset with the altitude and reaching a maximum deviation around 2.5 km above ground. The standard deviation increase with the altitude in the range 2-6 km for both retrievals, with a mean values of 1.9 K for the 8f-RET and 2.4 K for 12f-RET. From these results we can clearly observe a better agreement between the measurements from the radiosondes and the retrievals from TEMPERA when only the 8 more opaque channels are used under all weather conditions.

Lower bias and standard deviations are found in the PBL for the retrievals from HATPRO radiometer. The mean deviation ranges between -0.2 and 0.3 K in the first kilometer and between -0.5 and 1.2 K in the 1-2 km range altitude. Above 2 km the bias presents values between 0.5 and 1.5 K, showing a general decrease with the altitude. The standard deviation shows an increase with the altitude. The values ranges between 0.4 and 0.8 K in the first kilometer, 0.8 and 1.2 in the 1-2 km altitude range and a mean value of 1.5 K above 2 km.

In addition, we have assessed the accuracy of the retrievals only for clear-sky conditions. The clear cases have been selected using the product APCADA and the ILW from HATPRO as it was already indicated in previous sections. A total of 160 temperature profiles have been compared. Figure 7b shows the bias and the standard deviation for clear cases. For TEMPERA retrievals we can observe that although the bias is almost the same than for all weather condition in the first kilometer there are lower deviations above this altitude for both retrievals. The mean deviations range from -0.03 to 0.7 K and from 1.2 to 1.5 K in

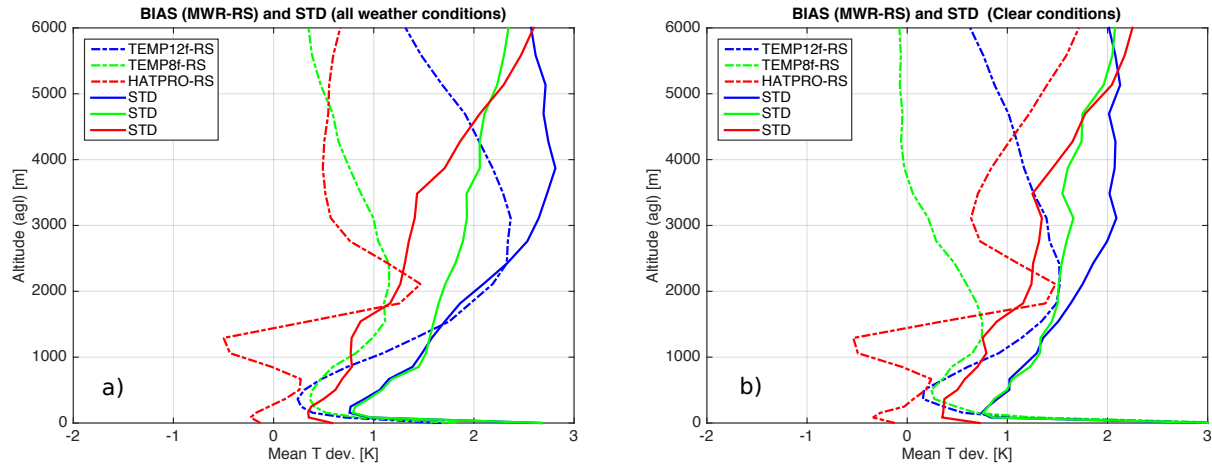


Figure 7. Mean and standard temperature deviation between HATPRO/TEMPERA radiometers and RSs for all weather conditions (a) and clear skies (b).

the altitude range between 2 and 4 km (agl), for 8f-RET and 12f-RET respectively. Above 4 km the bias is almost constant and close to zero (-0.1 K) for the 8f-RET and shows a positive mean bias of 0.9 K for the 12f-RET. The standard deviations for both retrievals show very similar values in the lower part than for all weather conditions (0.9 K of average in the first kilometer). Above this altitude the 8f-RET present lower standard deviation than 12f-RET (1.4 K against 1.6 K between 1 and 3 km, and 1.8 K against 2.1 K between 3 and 6 km). These results also evidence a better agreement between RS and TEMPERA when only 8 channels are used in the inversion algorithm although only clear cases have been selected. It could be explained for the larger Tb bias found for the most transparent channels under clear conditions.

The temperature comparison between HATPRO and RS under clear conditions shows almost identical values in the lowest part (from ground to 3 km) than for all weather conditions. The bias in this altitude range moves from -0.5 K at 1.3 km to 1.5 K at 2.1 km (agl). Above 3 km (agl) the mean bias is 1.3 K.

It is worth pointing out that the bias for 8f-RET from TEMPERA shows lower values than for HATPRO above 1.6 km (agl), although the standard deviation is slightly lower for HATPRO almost in the whole range.

We have classified the measurements between day and night cases in order to check if there was any temporal dependence. Figure 8 shows the bias and standard deviation for day (left) and night (right) measurements. We can observe that the standard deviations are very similar for all the retrievals in the lower troposphere (from ground to 2 km agl) during the day and nighttime. Slightly lower standard deviations are found above 2 km (agl) for the day-time retrievals from the two radiometers. In the case of the bias we can find some remarkable differences between day and night. We can observe a clear decrease in the bias for the retrievals from TEMPERA for day-time measurements. In the case of the 12f-RET is more evident, changing the maximum bias from 2.2 K for nighttime to 0.9 K for daytime. For the 8f-RET the decrease in the bias is also remarkable in

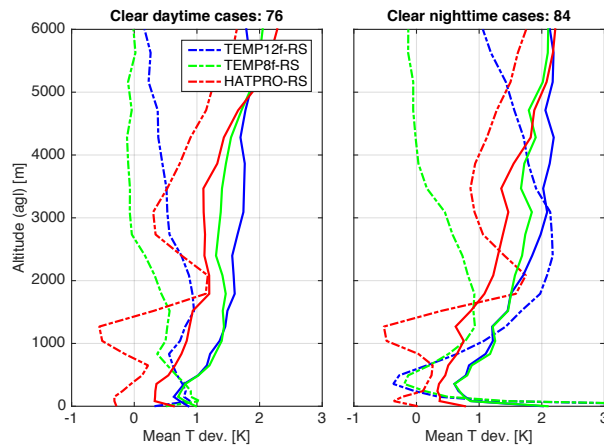


Figure 8. Mean and standard temperature deviation between HATPRO/TEMPERA radiometers and RSs during day (left) and night time (right) under clear conditions.

the altitude range from 1 to 4 km (agl). For this range, the mean deviation is 0.63 K during nighttime while it reaches a mean value 0.22 K during daytime.

It is worth mentioning that the differences between day and night-time deviations are much smaller for the retrievals from HATPRO. It could be explained because the inversion algorithm used for this radiometer is very well trained also for nighttime measurements, since the regression method was also trained with radiosondes launched during nighttime. The main remarkable atmospheric condition that can be found during the night is the presence of inversions. So, the results evidence a larger difficulty for the retrievals from TEMPERA, especially for the 12f-RET, under the presence of inversion layers. Löhnert and Maier (2012) also found discrepancies in the temperature bias during day and night-time. They found a non-zero behaviour as a function of height with opposite sign between both datasets. It is important to note that the temperature bias values found in that study for HATPRO were lower than the one observed in this work. It could be explained because they applied a Tb offset correction to that analysis.

6 Instrumental characteristic effect on microwave measurements

In this last section we assess the effect of instrumental characteristics such as the bandwidth of the individual filters and the antenna response on the brightness temperature.

Fig. 9 presents the possible errors caused by omitting the antenna pattern in measurement simulations. The Tb bias has been defined as the Tb calculated from ARTS model considering a pencil beam minus the simulated Tb including a beam width. The antenna pattern was considered simulating a Gaussian response with different HPBW (from 1° to 8°). The simulations have been calculated for the 12 frequencies of TEMPERA and a set of elevation angles which covers the observational angles



of both radiometers. From this plot we can observe that there is a strong dependency with frequency and the elevation angle. For the more opaque channels (> 55 GHz) the brightness temperatures saturate and the errors associated to the antenna pattern can be considered negligible. The effect of the antenna pattern is more evident for the most transparent channels. The errors are larger when a larger HPBW is considered to characterize the antenna response. Next we will mention the errors associated to a

5 HPBW of 4° , since the typical scanning radiometers used in the V-band have this or smaller beam widths. The smallest errors are found for the zenith observations, with maximum bias of -0.05 K at the frequency of 52.85 GHz. We can observe a similar behavior but with larger underestimation for lower elevation angles (up to 35°), at this angle the maximum bias reaches values of -0.07 K. We can observe that the deviations are much larger when a wider beam width is considered. For the elevation angle of 20° we observe a change in the tendency of the bias, where we can find an underestimation for the most transparent channels

10 (lower 52.5 GHz) and an overestimation above this frequency. The errors range between -0.3 K and $+0.1$ K. This change from negative to positive bias with the elevation angle was also observed by Meunier et al. (2013), and it is linked to a change in the curvature of the Tb curve. The errors become larger for lower elevation angles. A maximum overestimation of 0.4 K is found at 52.75 GHz for the elevation angle of 10.2° . The maximum errors are found in the lowest elevation angle with a bias that reaches 1.2 K in the most transparent channel. For this angle, it is worth to point out that the bias can reach values up to 3.5 K

15 for a beam width with 8° of HPBW. The larger deviation for the lowest elevation angle (5.4°) could be explained because the beam at least partially hits the ground (Meunier et al., 2013).

Figure 10 shows errors associated with the channel bandwidth effect in Tb differences for different elevation angles. The bias has been calculated as the Tb from ARTS model considering monochromatic receiver minus the simulated Tb considering different bandwidths (from 100 to 1000 MHz) and assuming a rectangular response. The 12 central frequencies used for

20 the simulations have been the ones corresponding to the TEMPERA's channels. From the plot we can clearly observe that the bandwidth effect is very small when the opacity is high, so it corresponds to frequencies above 55 GHz at all elevation angles. In contrast, the bandwidth can have an important effect for most transparent channels. A general feature observed from these simulations is the existence of an overestimation which moves up in frequency when the elevation angle increases. The maximum biases are found for the widest bandwidths and their values range between 0.9 and 3 K. This overestimation can

25 be explained by the positive curvature of the Tb spectrum existing for frequencies lower than in the saturation range (Fig. 2). Similar behavior has been observed by Meunier et al. (2013). For elevation angles larger than 10.2° we observe an underestimation present in most of the transparent channels. These negative biases reach the maximum values again for the widest bandwidth ranging from -0.6 K at 20° elevation angle to -1.8 K at the zenith observation. This negative bias is related with the negative Tb curve for the most transparent channels present when the opacity is not very high (larger elevation angles). It is

30 worth to point out the large bias observed for the two widest bandwidths (900 MHz and 1 GHz) at 5.4° elevation angle. While for the narrower bandwidths the deviations are smaller than 0.2 K for the widest ones reach biases which range between -1.7 and 3 K.

Meunier et al. (2013) found that over-estimations could reach values up to 8.5 K and -2.5 K for the under-estimation for the some frequencies with the 1 GHz bandwidth. These large deviations are caused when the peak of the oxygen individual

35 absorption lines are also covered by the bandwidth of one of the channels. For this reason is very important that the central

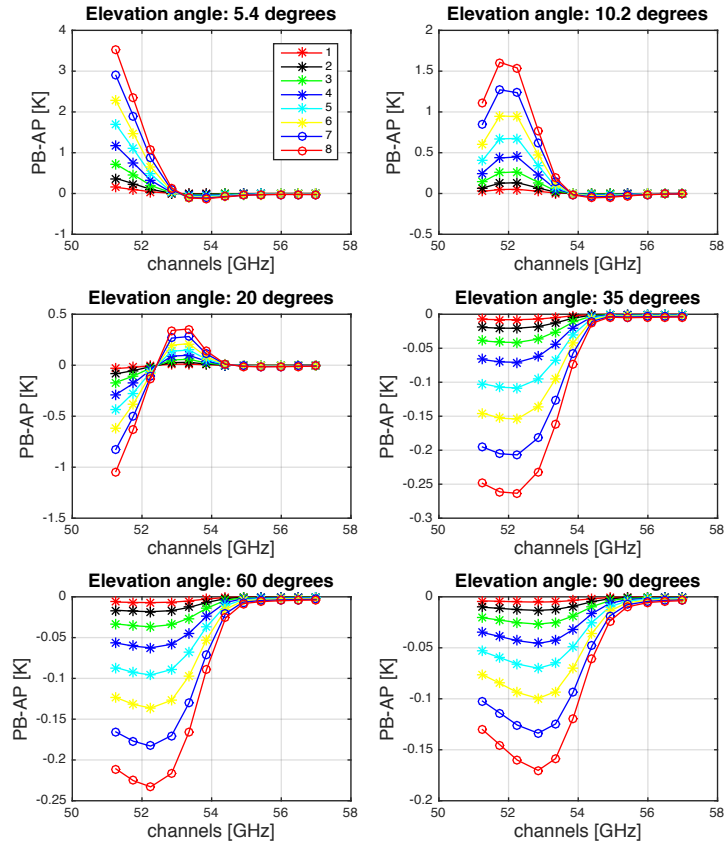


Figure 9. Errors associated to the antenna beam for different frequencies and elevation angles. The antenna beam was considered simulating a Gaussian response with different HPBW (from 1° to 8°). The biases have been calculated as the T_b s considering pencil beam (PB) minus the ones assuming different antenna patterns (AP).

frequencies and the bandwidths of the different radiometer filters are not in the frequency range of any of the multiple absorption peaks.

7 Conclusions

This work presents an assessment of the tropospheric performance of a new temperature radiometer (TEMPERA). This is the first temperature radiometer which measures tropospheric and stratospheric temperature at the same time. In this study the measured brightness temperature and the retrieved tropospheric temperature are assessed by means of a comparison with simultaneous and collocated radiosonde measurements. In addition, the TEMPERA performances are compared with the ones

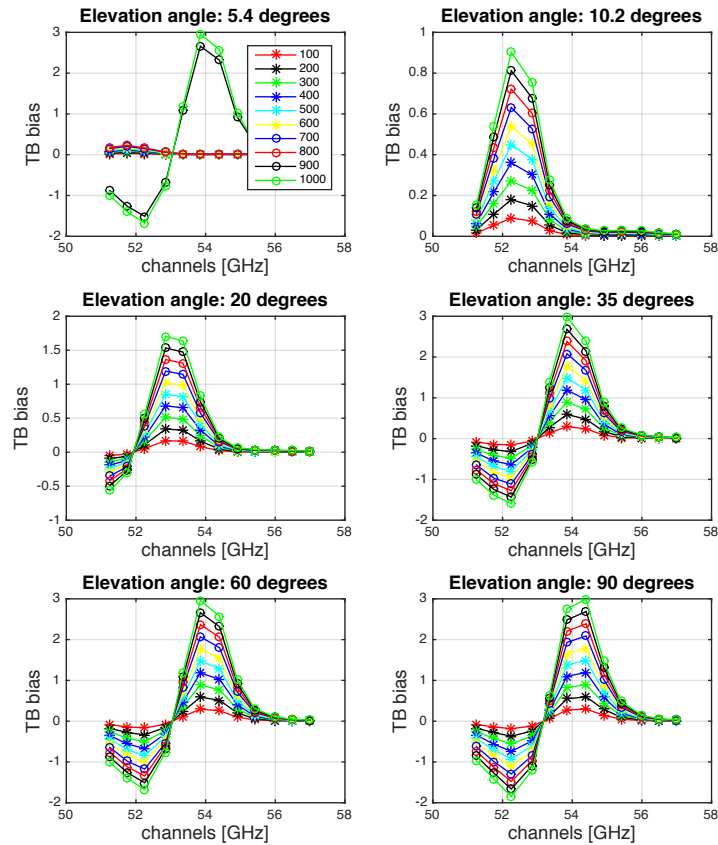


Figure 10. Errors associated with the bandwidth for different frequencies and elevation angles. The biases have been calculated as the Tb_s considering monochromatic receiver minus the ones assuming different bandwidths (from 100 to 1000 MHz).

from a commercial microwave radiometer (HATPRO) which has some different instrumental characteristics and uses a different inversion algorithm.

The measured brightness temperatures (Tb) from both radiometers (TEMPERA and HATPRO) have been compared with the ones simulated using radiosonde (RS) measurements. The simulated Tb from RS were calculated using the Atmospheric Radiative Transfer Simulator (ARTS). In general, much larger Tb deviations are found for the most transparent channels (<54 GHz) between the measured and the simulated Tb from RS for both radiometers. The deviations were much more pronounced for cloudy cases, where the bias reaches almost 20 K for some cases in the most transparent channels. The larger bias found for cloudy conditions can be explained by the presence of non homogeneous conditions for many of the cases, which cause that the measurements from different instruments are not comparable as they look not exactly to the same air volume.

10 In order to avoid the complexity of cloudy cases and to assess the effect due to instrumental and modeling aspects only cases with clear conditions were selected. For these conditions, most of the TEMPERA's channels showed a positive bias ranging



from 4.63 K for the most transparent channel and the lowest elevation angle to -1.1 K at the frequency of 52.85 GHz and the highest elevation angle (60°). The more opaque channels showed lower deviations ranging between 0.2 K and 1.3 K. Similar and even larger systematic offsets have been found in the more transparent V-band channels in other studies with radiometers from different manufacturers.

- 5 In the comparison between HATPRO and RS a similar pattern as for TEMPERA radiometer was found, with larger deviations for the most transparent channels. We observed a positive bias for all the frequencies and elevation angles except for the second channel (52.28 GHz). The positive bias ranged between 5.5 K and 0.8 K. The large negative deviation found for the second channel, which reached values up to -4 K, could be due to the fact that the central frequency defined for the model does not correspond to the actual center frequency the instrument is measuring.
- 10 Comparison of the retrieved temperature profiles evidenced a good agreement in general between both radiometers and the independent in-situ RS observations. Very similar values of mean deviations were found under all weather conditions between both retrievals calculated from TEMPERA measurements (with 8 and 12 channels) and the RS in the lowest troposphere (from ground to 1 km agl). The mean deviations were always lower than 0.86 K in this altitude range. Above 1 km lower mean deviations were found for 8f-RET with maximum bias of 1.2 K, while for 12 f-RET the maximum mean deviation reached 2.4
- 15 K at 2.5 km. The standard deviations were very similar for both retrievals in the lower part but they increased with the altitude resulting in larger deviations for 12f-RET.

Lower bias and standard deviations were found in the Planetary Boundary Layer for the retrievals from HATPRO radiometer. The mean deviation ranges between -0.2 and 0.3 K in the first kilometer and between -0.5 and 1.2 K in the 1-2 km range altitude. Above 2 km the bias presents values between 0.5 and 1.5 K, showing a general decrease with the altitude. The

20 standard deviation also shows an increase with the altitude but with lower values than for TEMPERA retrievals.

For clear cases the bias and the standard deviations were very similar for all the retrievals in the lower part of the troposphere, while the most remarkable effect was a decrease in the bias for all the radiometer retrievals above 2 km. It is worth to remark that the lowest bias above this altitude was found for the 8f-TEMPERA retrievals with values always lower than 0.6 K. The standard deviations also decreased specially for the 12f-RET.

- 25 A classification of the temperature profiles between day and night observations evidenced a decrease in the bias and standard deviation for the daytime observations. It was especially important for the TEMPERA retrievals, which presented lower bias than HATPRO in the far range (above 1.8 km). This comparison showed the good performance of HATPRO during nighttime measurements, where normally the presence of more complex situations such as inversions, fog, etc. could be present. In this sense, the fact that the linear regression method of HATPRO was trained with a large dataset of nighttime RS seems to be
- 30 crucial. The temperature value for TEMPERA at the lowest altitude could easily be improved by exchanging the retrieved value by a direct measurement of the temperature close to the instrument.

It is worth to point out the better agreement observed for TEMPERA when only the 8 more opaque channels were used in the temperature retrievals even under clear conditions. It could be due to the large deviations observed in the most transparent channels, which are also observed in other studies which used different radiative transfer models. In this sense, future efforts

35 should focus on the identification of the error sources of these uncertainties and in this way improve the performance of



these most transparent channels. Instrumental characteristics as the beamwidth and the bandwidth have been shown to have an important effect in the most transparent channels of the V-band, reaching values of up to 3 K in the case of the bandwidth. Other possible explanation could also be that spectroscopy is not yet fully understood.

We conclude that this study has shown the good performance of TEMPERA radiometer to determine the temperature in the troposphere. It is worth to remark the advantage of using the OEM for the TEMPERA retrievals which does not suffer the necessity of using a large RS database as is the case for linear regression or neuronal network methods.

Acknowledgements. This work has been funded by the Swiss National Science Foundation under grant 200020-160048 and MeteoSwiss in the framework of the GAW project "Fundamental GAW Parameters by Microwave Radiometry".



References

- Anderson, G. P., Clough, S., Kneizys, F., Chetwynd, J., and Shettle, E. P.: AFGL atmospheric constituent profiles (0.120 km), Tech. rep., DTIC Document, 1986.
- Bleisch, R., Kämpfer, N., and Haeferle, A.: Retrieval of tropospheric water vapour by using spectra of a 22 GHz radiometer, *Atmospheric Measurement Techniques*, 4, 1891–1903, doi:10.5194/amt-4-1891-2011, <http://www.atmos-meas-tech.net/4/1891/2011/>, 2011.
- 5 Buehler, S., Eriksson, P., Kuhn, T., Von Engel, A., and Verdes, C.: ARTS, the atmospheric radiative transfer simulator, *Journal of Quantitative Spectroscopy and Radiative Transfer*, 91, 65–93, 2005.
- Crewell, S. and Lohnert, U.: Accuracy of boundary layer temperature profiles retrieved with multifrequency multiangle microwave radiometry, *Geoscience and Remote Sensing, IEEE Transactions on*, 45, 2195–2201, 2007.
- 10 Dürr, B. and Philipona, R.: Automatic cloud amount detection by surface longwave downward radiation measurements, *Journal of Geophysical Research: Atmospheres* (1984–2012), 109, 2004.
- Eriksson, P., Buehler, S., Davis, C., Emde, C., and Lemke, O.: ARTS, the atmospheric radiative transfer simulator, version 2, *Journal of Quantitative Spectroscopy and Radiative Transfer*, 112, 1551–1558, 2011.
- Hewison, T. J., Cimini, D., Martin, L., Gaffard, C., and Nash, J.: Validating clear air absorption models using ground-based microwave radiometers and vice-versa, *Meteorologische Zeitschrift*, 15, 27–36, 2006.
- 15 Liebe, H., Hufford, G., and Cotton, M.: Propagation modeling of moist air and suspended water/ice particles at frequencies below 1000 GHz, in: *In AGARD, Atmospheric Propagation Effects Through Natural and Man-Made Obscurants for Visible to MM-Wave Radiation 11 p* (SEE N94-30495 08-32), vol. 1, 1993.
- Löhnert, U. and Crewell, S.: Accuracy of cloud liquid water path from ground-based microwave radiometry 1. Dependency on cloud model statistics, *Radio Sci*, 38, 8041, 2003.
- 20 Löhnert, U. and Maier, O.: Operational profiling of temperature using ground-based microwave radiometry at Payerne: prospects and challenges, *Atmospheric Measurement Techniques*, 5, 1121–1134, 2012.
- Martin, L., Schneebeli, M., and Matzler, C.: ASMUWARA, a ground-based radiometer system for tropospheric monitoring, *Meteorologische Zeitschrift*, 15, 11–17, 2006.
- 25 Meunier, V., Löhnert, U., Kollias, P., and Crewell, S.: Biases caused by the instrument bandwidth and beam width on simulated brightness temperature measurements from scanning microwave radiometers, *Atmospheric Measurement Techniques*, 6, 1171–1187, 2013.
- Navas-Guzmán, F., Stähli, O., and Kämpfer, N.: An integrated approach toward the incorporation of clouds in the temperature retrievals from microwave measurements, *Atmospheric Measurement Techniques*, 7, 1619–1628, 2014.
- Navas-Guzmán, F., Kämpfer, N., Murk, A., Larsson, R., Buehler, S., and Eriksson, P.: Zeeman effect in atmospheric O₂ measured by ground-based microwave radiometry, *Atmospheric Measurement Techniques*, 8, 1863–1874, 2015.
- 30 Rodgers, C. D.: *Inverse methods for atmospheric sounding: Theory and Practice*, Series on Atmospheric, Oceanic and Planetary Physics–Vol. 2, Singapore, World Scientific, 2000.
- Rose, T., Crewell, S., Löhnert, U., and Simmer, C.: A network suitable microwave radiometer for operational monitoring of the cloudy atmosphere, *Atmospheric Research*, 75, 183–200, 2005.
- 35 Rosenkranz, P.: *Absorption of microwaves by atmospheric gases*, 1993.
- Rosenkranz, P. W.: Water vapor microwave continuum absorption: A comparison of measurements and models, *Radio Science*, 33, 919–928, 1998.



Stähli, O., Murk, A., Kämpfer, N., Mätzler, C., and Eriksson, P.: Microwave radiometer to retrieve temperature profiles from the surface to the stratopause, *Atmospheric Measurement Techniques*, 6, 2477–2494, 2013.

Ware, R., Carpenter, R., Güldner, J., Liljegren, J., Nehr Korn, T., Solheim, F., and Vandenberghe, F.: A multichannel radiometric profiler of temperature, humidity, and cloud liquid, *Radio Science*, 38, 8079, 2003.